A centered second-order finite volume scheme for the heterogeneous Maxwell equations in three dimensions on arbitrary unstructured meshes

Serge Piperno[1]   Malika Remaki   Loula Fezoui

Abstract

Nous dmontrons une condition de stabilit L^2 de type CFL pour un schma en volumes finis du second-ordre propos par Remaki pour la rsolution des quations de Maxwell en domaine temporel, en milieu htrogne et avec des conditions aux limites mtalliques ou absorbantes. Nous donnons une condition suffisante de stabilit de forme trs gnrale, valide pour des partitions en volumes finis arbitraires, en deux ou trois dimensions d'espace. Des simulations numriques montrent le potentiel de cette nouvelle mthode.

Un schma en volumes-finis non-structurs centr et du second-ordre pour la rsoluttion des quations de Maxwell tridimensionnelles en milieu htrogne

Résumé

We prove a sufficient CFL-like condition for the L^2 stability of the second-order accurate finite volume scheme proposed by Remaki for the time-domain solution of Maxwell equations in heterogenous media, with metallic and absorbing boundary conditions. We yield a very general sufficient condition, valid for any finite volume partition in two and three space dimensions. Numerical tests show the potential of this original finite volume scheme in one, two and three space dimensions for the numerical solution of Maxwell equations in the time domain.

[1]CERMICS, INRIA, BP93, F-06902 Sophia-Antipolis Cedex, Serge.Piperno@sophia.inria.fr

Contents

1 Introduction

The modeling of systems involving electromagnetic waves has known a kind of "reinvention" [24] through the resolution of the time-domain Maxwell equations on space grids. Many different types of methods have been used. Finite Difference Time-Domain (FDTD) methods (based on Yee's scheme [30] or on implicit time schemes [21]), are efficient mostly on structured regular grids, whereas finite element methods, based on unstructured meshes, can deal with naturally complex geometries [8], but induce heavy computations of mass matrices. Gathering many advantages, Finite Volume Time-Domain (FVTD)methods can also be based on unstructured meshes and get rid of differential operators (and finite element mass matrices) using Green's formula for the integration over finite volumes (see [9] for a review of numerical methods used in Computational Electromagnetics and [25] for an accurate review of FDTD and FVTD methods).

We are interested here in FVTD methods, as have been developed in the past years, not necessarily on body-fitted coordinates [22, 23] but on unstructured finite element triangulations [6, 7, 8, 20] or on totally destructured meshes [3]. More precisely, we consider a standard finite volume approximation, i.e. a piecewise constant, discontinuous, Galerkin-type finite element approximation [14]. As the Maxwell system in transient state is hyperbolic and may be rewritten in conservative form, it is natural to use a numerical approximation based on conservative schemes, in a first step directly inspired by previous works in the field of Computational Fluid Dynamics. The convergence of first-order conservative upwind schemes has been established for different hyperbolic equations in any dimension [11], and L^1 error estimates of $h^{1/2}$ (where h is a characteristic mesh size) have been proved recently for a general hyperbolic equation [27].

The stability of finite volume schemes has been investigated since many years, for regular grids using the Von Neumann analysis [1] or the modified equation analysis [29]. Both analyses do not deal either with boundary conditions or with non regular grids. The concept of Total Variation Diminishing (TVD) scheme, proposed by Harten [12], leads to L^∞-stability results for finite volume schemes on non regular grids only in one space dimension, and can be related to the idea of Local Extremum Diminishing (LED) scheme, proposed by Jameson [13], which extends some properties to several dimensions. In a previous paper [17], we have investigated the L^2-stability of first-order upwind finite volume schemes in two and three space dimensions on unstructured meshes, for the numerical solution of the time-domain Maxwell equations. Quasi-optimal sufficient stability conditions were obtained on arbitrary finite-volume partitions, which were mentioned and actually used [3], and which extend a general condition derived for Friedrichs' systems in general [28].

However, upwind schemes are very disappointing when used for the numerical simulation of electromagnetic waves propagation, since the numerical diffusion induced by upwinding − necessary in Computational Fluid Dynamics to limit unphysical oscillations − makes long-run computations (at least over several periods) very inaccurate. In this paper, we investigate a new finite volume method proposed by Remaki [19] for the numerical solution of Maxwell equations in heterogeneous media. In that heterogeneous framework, a result of existence and uniqueness of the solution is now available [18]. Remaki's FVTD method is based on a second-order leap-frog time scheme and on second-order centered numerical fluxes. This scheme yields a original conservative finite volume method, with no numerical diffusion. Finite volumes of arbitrary shape are considered, as well as two types of boundary conditions (absorbing and metallic boundary conditions). As done previously for upwind schemes on arbitrary meshes, an energy-type method, drawn from some finite element proofs [5], is used to prove the L^2-stability of the scheme.

This paper is organized has follows. In section 2, we introduce a pseudo-conservative form of Maxwell equations in three dimensions for heterogeneous media, We also introduce some notations. In section 3, we recall the centered leap-frog second-order finite-volume scheme proposed by Remaki for the time domain solution of Maxwell equations. In section 4, we prove the sufficient stability condition for this scheme. This proof is based on the definition of a discrete electromagnetic energy. We also prove in this section that this energy is exactly conserved if no absorbing boundaries are present. Finally, we present in section 5 some numerical results in two and three dimensions, both for homogeneous and heterogeneous media.

2 The heterogeneous 3D Maxwell equations

We consider Maxwell equations in three space dimensions (heterogeneous linear isotropic medium with no source, with space varying electric permittivity $\epsilon(x)$ and magnetic permeability $\mu(x)$, the local light speed $c(x)$ being given by $\epsilon(x)\mu(x)c(x)^2 = 1$). The electric field $E = {}^t(E_x, E_y, E_z)$ and the magnetic field $H = {}^t(H_x, H_y, H_z)$ verify

$$\begin{cases} \epsilon \dfrac{\partial E}{\partial t} = \nabla \times H, \\ \mu \dfrac{\partial H}{\partial t} = -\nabla \times E. \end{cases}$$

These equations are set in a bounded polyhedral domain Ω of $\mathbb{R}^3$. Everywhere on the domain boundary $\partial\Omega$, exactly one of the two possible boundary conditions is set: a metallic boundary condition (on $\partial\Omega_m$, around a metallic object or inside a cavity for example) or an absorbing boundary condition (on $\partial\Omega_a$, possibly on the outer boundary of the domain $\partial\Omega_\infty$, see Figure 1).
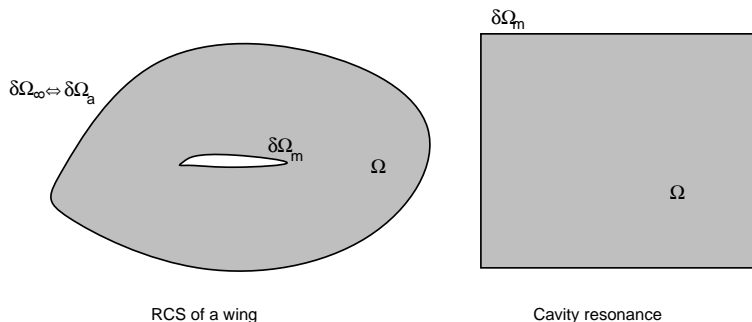

Figure 1: Domain Ω and domain boundary

In three space dimensions, the metallic boundary condition writes $\vec{n} \times E = \vec{0}$, with $\vec{n}$ the unitary outwards normal. In the following, a first-order Silver-Mller absorbing condition is used on the absorbing boundary $\partial\Omega_a$, which writes

$$\vec{n} \times E = -c\mu \ \vec{n} \times (\vec{n} \times H). \tag{1}$$

The Maxwell system can be transformed into a pseudo-conservative form:

$$\begin{cases} \epsilon \dfrac{\partial E}{\partial t} + N_x \dfrac{\partial H}{\partial x} + N_y \dfrac{\partial H}{\partial y} + N_z \dfrac{\partial H}{\partial z} &= 0, \\ \mu \dfrac{\partial H}{\partial t} - N_x \dfrac{\partial E}{\partial x} - N_y \dfrac{\partial E}{\partial y} - N_z \dfrac{\partial E}{\partial z} &= 0, \end{cases} \tag{2}$$

where the anti-symmetric matrices N_x, N_y and N_z are given by

$$N_x = \begin{pmatrix} 0 & 0 & 0 \\ 0 & 0 & 1 \\ 0 & -1 & 0 \end{pmatrix}, \quad N_y = \begin{pmatrix} 0 & 0 & -1 \\ 0 & 0 & 0 \\ 1 & 0 & 0 \end{pmatrix}, \quad N_z = \begin{pmatrix} 0 & 1 & 0 \\ -1 & 0 & 0 \\ 0 & 0 & 0 \end{pmatrix}.$$

For any vector $\vec{n} = {}^t(n_x, n_y, n_z)$, the matrix $N_{\vec{n}} = n_x N_x + n_y N_y + n_z N_z$ is anti-symmetric and operates as $N_{\vec{n}} X = -\vec{n} \times X$.

3 The centered leap-frog FVTD method

3.1 Introduction

We assume we dispose of an arbitrary partition of the domain Ω into a finite number of connected polyhedral finite volumes (each one with a finite number of faces). For example, this assumption covers

the two cases of vertex-centered and element-centered finite volumes [7]. For each finite volume or "cell" $\mathcal{T}_i$, V_i denotes its volume, and ϵ_i and μ_i are respectively the local electric permittivity and magnetic permeability of the medium, which are assumed constant in the cell $\mathcal{T}_i$.

We call interface between two finite volumes their intersection, whenever it is a polyhedral surface. For each internal interface $a_{ij} = \mathcal{T}_i \bigcap \mathcal{T}_j$, we denote by $\vec{n}_{ij} = {}^t(n_{ijx}, n_{ijy}, n_{ijz})$ the integral over the interface of the unitary normal, oriented from $\mathcal{T}_i$ towards $\mathcal{T}_j$. The same definitions are extended to boundary interfaces (in the intersection of the domain boundary $\partial\Omega_m \bigcup \partial\Omega_a$ with a boundary finite volume), the index j corresponding to a fictitious cell outside the domain. We denote by $\vec{\tilde{n}}_{ij} = {}^t(\tilde{n}_{ijx}, \tilde{n}_{ijy}, \tilde{n}_{ijz})$ the normalized normals $\vec{\tilde{n}}_{ij} = \vec{n}_{ij}/\|\vec{n}_{ij}\|$. For the sake of simplicity, we use the notations $N_{ij} = N_{\vec{n}_{ij}} = \|\vec{n}_{ij}\|\, N_{\vec{\tilde{n}}_{ij}}$.

Finally, we denote by $\mathcal{V}_i$ the set of indices of the neighboring finite volumes of the finite volume $\mathcal{T}_i$ (having an interface in common). We denote by P_i the discrete measure of the boundary of a finite volume cell, which is defined by

$$P_i = \sum_{j \in \mathcal{V}_i} \|\vec{n}_{ij}\|. \tag{3}$$

3.2 Conservative finite volume scheme

The conservative finite volume scheme proposed by Remaki [19] is written:

$$\begin{cases} \epsilon_i V_i \dfrac{E_i^{n+1} - E_i^n}{\Delta t} + \displaystyle\sum_{j \in \mathcal{V}_i} F_{ij}^{n+1/2} = 0, \\[2ex] \mu_i V_i \dfrac{H_i^{n+3/2} - H_i^{n+1/2}}{\Delta t} - \displaystyle\sum_{j \in \mathcal{V}_i} G_{ij}^{n+1} = 0, \end{cases} \tag{4}$$

where the index i is linked to the cell $\mathcal{T}_i$, Δt is the time step, E_i^n (resp. $H_i^{n+1/2}$) is an approximate for the average of the electric (resp. magnetic) field over the cell $\mathcal{T}_i$ at time $t^n = n\,\Delta t$ (resp. $t^{n+1/2} = (n+\frac{1}{2})\,\Delta t$). The word average has to be understood as a space-mean value, which is defined for any field X and each cell $\mathcal{T}_i$ by

$$X_i = \frac{1}{V_i} \int_{\mathcal{T}_i} X(s)\, ds.$$

Finally, $F_{ij}^{n+1/2}$ and G_{ij}^{n+1} are centered numerical fluxes. The reader can check that the finite volume scheme (4) is written as a leap-frog scheme: numerical values E_i^n and $H_i^{n+1/2}$ are used in numerical fluxes to obtain a new set of numerical values E_i^{n+1} and $H_i^{n+3/2}$.

The numerical fluxes are defined as follows:

- the fluxes $F_{ij}^{n+1/2}$ and G_{ij}^{n+1} are given for internal interfaces by

$$F_{ij}^{n+1/2} = N_{ij}\, \frac{H_i^{n+1/2} + H_j^{n+1/2}}{2}, \quad G_{ij}^{n+1} = N_{ij}\, \frac{E_i^{n+1} + E_j^{n+1}}{2}. \tag{5}$$

- for a metallic boundary interface, we use the following numerical fluxes:

$$F_{ij}^{n+1/2} = N_{ij}\, H_i^{n+1/2}, \quad G_{ij}^{n+1} = 0, \tag{6}$$

which could be obtained using a fictitious cell with $H_j^{n+1/2} = H_i^{n+1/2}$ and $E_j^{n+1} = -E_i^{n+1}$. The choice for G_{ij}^{n+1} is clearly a second-order approximation of the condition $\vec{n} \times E = 0$ at the interface, whereas the choice for $F_{ij}^{n+1/2}$ is classically used in FDTD methods. For Maxwell equations in one-dimension, this weak treatment leads to an accurate reflection of incoming waves.

- finally, for an interface a_{ij} on the absorbing boundary Ω_a, the numerical fluxes $F_{ij}^{n+1/2}$ and G_{ij}^{n+1} will be detailed in the sequel.

4

3.3 Matricial properties

The following elementary equalities hold:

$$\vec{n}_{ji} = -\vec{n}_{ij}, \qquad N_{ji} = -N_{ij}. \tag{7}$$

At the same time, geometrical properties hold for each cell $\mathcal{T}_i$:

$$\sum_{\text{interfaces of } \mathcal{T}_i} \vec{n}_{ij} = \vec{0}, \qquad \sum_{\text{interfaces of } \mathcal{T}_i} N_{ij} = 0. \tag{8}$$

4 A sufficient stability condition

4.1 Energy estimates

We aim at giving and proving a necessary and/or sufficient condition for the L^2-stability of the finite volume scheme (4-5-6) with absorbing boundary fluxes to be determined. We use the same kind of energy approach as in [17], where a quadratic form plays the role of a Lyapunov function of the whole set of numerical unknowns. We first propose the following discrete energy, directly derived from the expression of the total numerical electromagnetic energy:

$$\mathcal{E}^n = \sum_i V_i \left(\epsilon_i \,^t E_i^n E_i^n + \mu_i \,^t H_i^{n-1/2} H_i^{n+1/2} \right). \tag{9}$$

We recall here that the electromagnetic energy in the continuous case verifies some conservation equation (Poynting's theorem) for the Maxwell system with no current. This theorem states that

$$\int_V \frac{\partial \mathcal{E}}{\partial t} dx + \int_{\partial V} \vec{P} \cdot \vec{n} ds = 0,$$

for any closed volume V with a regular boundary ∂V, where W the electromagnetic energy (for an isotropic medium) and Poynting's vector $\vec{P}$ are respectively given by

$$\mathcal{E} = \frac{1}{2}\varepsilon E^2 + \frac{1}{2}\mu H^2, \quad \vec{P} = E \times H.$$

For a given metallic cavity, since $E \times n = 0$ at the boundary, Poynting's theorem yields that the electromagnetic energy is exactly conserved in the cavity. Following this idea, we naturally try to use the proposed discrete energy (9) as a Lyapunov function.

It is absolutely not obvious why the discrete energy (9) should be a positive definite quadratic form of all numerical unknowns (let us say, the E_i^n and the $H_i^{n-1/2}$). We notice here that the situation is quite different from the proof of the L^2-stability of the first-order upwind finite-volume scheme of [17], where the energy was obviously a positive definite quadratic form of all unknowns. At the same time, the energy proposed here depends explicitly on the numerical scheme, since it can be only written as a quadratic form of all unknowns $(E_i^n, H_i^{n-1/2})$ through the use of the second part of the scheme (4). Finally, the variation of this discrete energy during a time step might lead to tedious computations, as for the first-order upwind scheme.

In the following, we shall prove that the proposed energy, with additional boundary correction terms, is **both non-increasing** during a time step **and a positive definite quadratic form of all unknowns** under a CFL-like condition on the time-step Δt. This will yield the proof that the scheme is L^2-stable (with the proposed energy) under a stability condition on Δt.

We propose for the energy variation $\Delta \mathcal{E} = \mathcal{E}^{n+1} - \mathcal{E}^n$ the

LEMMA 4.1 *Using the scheme (4-5-6), with some absorbing boundary fluxes $F_{ij}^{n+1/2}$ and G_{ij}^{n+1} (to be defined), we have the following estimation for $\Delta \mathcal{E}$:*

$$\Delta \mathcal{E} = \Delta t \sum_{\substack{interfaces}}^{absorbing} \left[-\,^t\!\left(E_i^n + E_i^{n+1} \right) \left(F_{ij}^{n+1/2} - N_{ij} H_i^{n+1/2} \right) + \,^t H_i^{n+1/2} (G_{ij}^n + G_{ij}^{n+1}) \right].$$

Proof: We have:

$$\Delta\mathcal{E} = \sum_i {}^t\!\left(E_i^n + E_i^{n+1}\right)\left[\epsilon_i V_i (E_i^{n+1} - E_i^n)\right] + \mu_i V_i {}^t\!H_i^{n+1/2}\left[H_i^{n+3/2} - H_i^{n+1/2} + H_i^{n+1/2} - H_i^{n-1/2}\right]$$

$$= \Delta t \sum_i \sum_{j\in\mathcal{V}_i}\left[-{}^t\!\left(E_i^n + E_i^{n+1}\right)F_{ij}^{n+1/2} + {}^t\!H_i^{n+1/2}\left(G_{ij}^n + G_{ij}^{n+1}\right)\right].$$

All terms in the double summation above correspond to finite volume interfaces. These terms can then be distributed on volume interfaces. We have:

$$\Delta\mathcal{E} = \Delta t \cdot \left(T_{\text{internal}} + T_{\text{metallic}} + T_{\text{absorbing}}\right), \quad \text{with}$$

$$T_{\text{internal}} = \sum_{\substack{\text{internal}\\\text{interfaces}}}\left[-{}^t\!\left(E_i^n + E_i^{n+1}\right)F_{ij}^{n+1/2} - {}^t\!\left(E_j^n + E_j^{n+1}\right)F_{ji}^{n+1/2}\right.$$
$$\left. +{}^t\!H_i^{n+1/2}(G_{ij}^n + G_{ij}^{n+1}) + {}^t\!H_j^{n+1/2}(G_{ji}^n + G_{ji}^{n+1})\right],$$

$$T_{\text{metallic}} = \sum_{\substack{\text{metallic}\\\text{interfaces}}}\left[-{}^t\!\left(E_i^n + E_i^{n+1}\right)F_{ij}^{n+1/2} + {}^t\!H_i^{n+1/2}(G_{ij}^n + G_{ij}^{n+1})\right],$$

$$T_{\text{absorbing}} = \sum_{\substack{\text{absorbing}\\\text{interfaces}}}\left[-{}^t\!\left(E_i^n + E_i^{n+1}\right)F_{ij}^{n+1/2} + {}^t\!H_i^{n+1/2}(G_{ij}^n + G_{ij}^{n+1})\right].$$

For the internal interface term, we can replace the centered numerical fluxes by the formula (5). Using the identities ${}^t\!N_{ij} = -N_{ij} = N_{ji}$, we find:

$$T_{\text{internal}} = \sum_{\substack{\text{internal}\\\text{interfaces}}}\left[{}^t\!H_i^{n+1/2}N_{ij}\left(E_i^n + E_i^{n+1}\right) + {}^t\!H_j^{n+1/2}N_{ji}\left(E_j^n + E_j^{n+1}\right)\right].$$

For the metallic interface term, we can replace the metallic fluxes by the formula (6). We easily find:

$$T_{\text{metallic}} = \sum_{\substack{\text{metallic}\\\text{interfaces}}}\left[{}^t\!H_i^{n+1/2}N_{ij}\left(E_i^n + E_i^{n+1}\right)\right].$$

Finally, we find that many terms vanish, since

$$\sum_{\substack{\text{absorbing}\\\text{interfaces}}}\left[{}^t\!H_i^{n+1/2}N_{ij}\left(E_i^n + E_i^{n+1}\right)\right] + T_{\text{metallic}} + T_{\text{internal}} =$$

$$\sum_{\substack{\text{internal}\\\text{interfaces}}}\left[{}^t\!H_i^{n+1/2}N_{ij}\left(E_i^n + E_i^{n+1}\right) + {}^t\!H_j^{n+1/2}N_{ji}\left(E_j^n + E_j^{n+1}\right)\right] +$$

$$\sum_{\substack{\text{metallic}\\\text{interfaces}}}\left[{}^t\!H_i^{n+1/2}N_{ij}\left(E_i^n + E_i^{n+1}\right)\right] + \sum_{\substack{\text{absorbing}\\\text{interfaces}}}\left[{}^t\!H_i^{n+1/2}N_{ij}\left(E_i^n + E_i^{n+1}\right)\right] =$$

$$\sum_i\left[\sum_{j\in\mathcal{V}_i}{}^t\!H_i^{n+1/2}N_{ij}\left(E_i^n + E_i^{n+1}\right)\right] = \sum_i\left[{}^t\!H_i^{n+1/2}\left(\sum_{j\in\mathcal{V}_i}N_{ij}\right)\left(E_i^n + E_i^{n+1}\right)\right] = 0.$$

We then have

$$\Delta\mathcal{E} = \Delta t\sum_{\substack{\text{absorbing}\\\text{interfaces}}}\left[-{}^t\!\left(E_i^n + E_i^{n+1}\right)\left(F_{ij}^{n+1/2} - N_{ij}H_i^{n+1/2}\right) + {}^t\!H_i^{n+1/2}(G_{ij}^n + G_{ij}^{n+1})\right],$$

which is exactly the result of the lemma.

The lemma above shows that the energy variation is only due to absorbing boundaries. One consequence is that with only metallic boundaries, the discrete energy is exactly conserved. We can notice that we recover the exact conservation of the electromagnetic energy of the continuous case for a metallic cavity. If some absorbing boundary conditions are present, in view of the result of the preceding lemma, we can now propose some choices for the absorbing boundary fluxes $F_{ij}^{n+1/2}$ and G_{ij}^{n+1}:

$$
\begin{cases}
F_{ij}^{n+1/2} = \dfrac{N_{ij}}{2} H_i^{n+1/2} + \sqrt{\dfrac{\epsilon_i}{\mu_i}} \dfrac{\|\vec{n}_{ij}\|}{2} E_{iT_{ij}}^{n}, & \text{with } E_{iT_{ij}}^{n} = E_i^n - \left({}^t\vec{n}_{ij}.E_i^n \right) \vec{n}_{ij}, \\[3mm]
G_{ij}^{n+1} = \dfrac{N_{ij}}{2} E_i^{n+1} - \sqrt{\dfrac{\mu_i}{\epsilon_i}} \dfrac{\|\vec{n}_{ij}\|}{2} H_{iT_{ij}}^{n+1/2}, & \text{with } H_{iT_{ij}}^{n+1/2} = H_i^{n+1/2} - \left({}^t\vec{n}_{ij}.H_i^{n+1/2} \right) \vec{n}_{ij}.
\end{cases}
\tag{10}
$$

In these definitions, $E_{iT_{ij}}^{n}$ and $H_{iT_{ij}}^{n+1/2}$ are respectively the tangential (orthogonally to the normal $\vec{n}_{ij}$) parts of the vectors E_i^n and $H_i^{n+1/2}$. The reader can also notice that the fields E_i^n and $H_i^{n+1/2}$ are available when the boundary flux $F_{ij}^{n+1/2}$ is used, and then that the fields E_i^{n+1} and $H_i^{n+1/2}$ are also available when the boundary flux G_{ij}^{n+1} is used.

The origin of these fluxes might seem not really obvious. In fact, they correspond to upwind fluxes at the absorbing boundary. More precisely, the reader can check that the flux $F_{ij}^{n+1/2}$ proposed above corresponds to the three electric field components of the six-component upwind flux $M_{ij}^{+\,t}\!\left(E_i^n, H_i^{n+1/2}\right)$, where $M_{ij} = A_x n_{ij_x} + A_y n_{ij_y} + A_z n_{ij_z}$, the matrices A_x, A_y, A_z correspond to the operators in the conservative form of the Maxwell equations in function of the complete electromagnetic field ${}^t(E, H)$, and the superscript $^+$ corresponds to the positive part via diagonalization of a matrix (see [17] for complete details). Similarly, G_{ij}^{n+1} corresponds to the three magnetic components of the six-component upwind flux $M_{ij}^{+\,t}\!\left(E_i^{n+1}, H_i^{n+1/2}\right)$.

The reader can notice that these fluxes lead to a genuinely first-order treatment of the absorbing condition, since the approximation is first order both in space (upwind fluxes) and in time ($F_{ij}^{n+1/2}$ is based on E_i^n and G_{ij}^{n+1} on $H_i^{n+1/2}$). With some time-interpolation, these fluxes can be corrected to reach second-order accuracy for Maxwell equations in one dimension. We plan to compare these treatments of the absorbing condition with Berenger's Perfectly Matched Layers [4], which are largely used in computational electromagnetics simulations [2, 10, 16, 15]. However, our main goal here is to get a stability result, and we are actually able to reach that goal only for these first-order accurate absorbing fluxes, as will be shown in the sequel.

With the choice (10) for the boundary fluxes, a value for the variation $\Delta\mathcal{E}$ of the discrete energy (9) deriving from Lemma 4.1 is given in the

LEMMA 4.2 *Using the scheme (4-5-6-10), we have the following estimation for $\Delta\mathcal{E}$:*

$$
\Delta\mathcal{E} = -\Delta t \sum_{\substack{interfaces \\ }}^{absorbing} \frac{\|\vec{n}_{ij}\|}{2} \left[\sqrt{\frac{\epsilon_i}{\mu_i}} \, {}^t E_{iT_{ij}}^{n} \; \left(E_{iT_{ij}}^{n} + E_{iT_{ij}}^{n+1} \right) + \sqrt{\frac{\mu_i}{\epsilon_i}} \, {}^t H_{iT_{ij}}^{n+1/2} \; \left(H_{iT_{ij}}^{n-1/2} + H_{iT_{ij}}^{n+1/2} \right) \right]
$$

Proof: Lemma 4.1 yields

$$\Delta\mathcal{E} \;=\; \Delta t \sum_{\substack{\text{interfaces}}}^{\text{absorbing}} \left[-{}^t\!\left(E_i^n + E_i^{n+1}\right)\left(F_{ij}^{n+1/2} - N_{ij}H_i^{n+1/2}\right) + {}^t\!H_i^{n+1/2}(G_{ij}^n + G_{ij}^{n+1})\right]$$

$$=\; \Delta t \sum_{\substack{\text{interfaces}}}^{\text{absorbing}} \left[{}^t\!\left(E_i^n + E_i^{n+1}\right)\frac{N_{ij}}{2}H_i^{n+1/2} - {}^t\!\left(E_i^n + E_i^{n+1}\right)\sqrt{\frac{\epsilon_i}{\mu_i}}\,\frac{\|\vec{n}_{ij}\|}{2}E_{i\,T_{ij}}^{\,n} \right.$$

$$\left. +\; {}^t\!H_i^{n+1/2}\frac{N_{ij}}{2}\left(E_i^n + E_i^{n+1}\right) - {}^t\!H_i^{n+1/2}\sqrt{\frac{\mu_i}{\epsilon_i}}\,\frac{\|\vec{n}_{ij}\|}{2}(H_{i\,T_{ij}}^{\,n\text{-}1/2} + H_{i\,T_{ij}}^{\,n+1/2})\right]$$

$$=\; -\Delta t \sum_{\substack{\text{interfaces}}}^{\text{absorbing}} \frac{\|\vec{n}_{ij}\|}{2}\left[\sqrt{\frac{\epsilon_i}{\mu_i}}\,{}^tE_{i\,T_{ij}}^{\,n}\,(E_{i\,T_{ij}}^{\,n} + E_{i\,T_{ij}}^{\,n+1}) + \sqrt{\frac{\mu_i}{\epsilon_i}}\,{}^tH_{i\,T_{ij}}^{\,n+1/2}\,(H_{i\,T_{ij}}^{\,n\text{-}1/2} + H_{i\,T_{ij}}^{\,n+1/2})\right]$$

which is the result of the lemma.

4.2   A corrected discrete energy

The discrete energy $\mathcal{E}^n$ proposed in (9) depends explicitly on the "updating scheme" for the magnetic field, and therefore on the particular choice for G_{ij}^{n+1}. Then it is not really surprising that this energy will have to be corrected to help us in our proof. Let us then introduce a corrected discrete energy $\mathcal{F}^n$, given by

$$\mathcal{F}^n = \mathcal{E}^n - \Delta t \sum_{\substack{\text{interfaces}}}^{\text{absorbing}} \frac{\|\vec{n}_{ij}\|}{4}\left[\sqrt{\frac{\epsilon_i}{\mu_i}}\,\|E_{i\,T_{ij}}^{\,n}\|^2 - \sqrt{\frac{\mu_i}{\epsilon_i}}\,\|H_{i\,T_{ij}}^{\,n\text{-}1/2}\|^2\right]. \tag{11}$$

The physical meaning of this corrected discrete energy is not straightforward. Correction terms are only related to absorbing boundaries (which means that $\mathcal{F}^n = \mathcal{E}^n$ if there are none). The additional terms probably find their origin in the temporal inconsistency of boundary numerical fluxes.

We can now prove that the discrete energy $\mathcal{F}^n$ is non-increasing, when our centered finite volume scheme is used. This is summed up in the following

LEMMA 4.3 *Using the scheme (4-5-6-10), the discrete energy $\mathcal{F}^n$ given by (9-11) is non-increasing. More precisely, the energy variation $\Delta\mathcal{F} = \mathcal{F}^{n+1} - \mathcal{F}^n$ is given by*

$$\Delta\mathcal{F} = -\Delta t \sum_{\substack{\text{interfaces}}}^{\text{absorbing}} \|\vec{n}_{ij}\|\left[\sqrt{\frac{\epsilon_i}{\mu_i}}\left\| \frac{E_{i\,T_{ij}}^{\,n} + E_{i\,T_{ij}}^{\,n+1}}{2}\right\|^2 + \sqrt{\frac{\mu_i}{\epsilon_i}}\left\| \frac{H_{i\,T_{ij}}^{\,n\text{-}1/2} + H_{i\,T_{ij}}^{\,n+1/2}}{2}\right\|^2\right] \leq 0.$$

Proof: The proof is elementary. We simply add terms deriving from the correction in $\mathcal{F}^n$ to the result of Lemma 4.2 for $\Delta\mathcal{E}$. We have

$$\Delta\mathcal{F} \;=\; -\Delta t \sum_{\substack{\text{interfaces}}}^{\text{absorbing}} \frac{\|\vec{n}_{ij}\|}{2}\left[\sqrt{\frac{\epsilon_i}{\mu_i}}\,{}^tE_{i\,T_{ij}}^{\,n}\,(E_{i\,T_{ij}}^{\,n} + E_{i\,T_{ij}}^{\,n+1}) + \sqrt{\frac{\mu_i}{\epsilon_i}}\,{}^tH_{i\,T_{ij}}^{\,n+1/2}\,(H_{i\,T_{ij}}^{\,n\text{-}1/2} + H_{i\,T_{ij}}^{\,n+1/2})\right]$$

$$-\;\Delta t \sum_{\substack{\text{interfaces}}}^{\text{absorbing}} \frac{\|\vec{n}_{ij}\|}{4}\left[\sqrt{\frac{\epsilon_i}{\mu_i}}\,\|E_{i\,T_{ij}}^{\,n+1}\|^2 - \sqrt{\frac{\mu_i}{\epsilon_i}}\,\|H_{i\,T_{ij}}^{\,n+1/2}\|^2\right]$$

$$+\;\Delta t \sum_{\substack{\text{interfaces}}}^{\text{absorbing}} \frac{\|\vec{n}_{ij}\|}{4}\left[\sqrt{\frac{\epsilon_i}{\mu_i}}\,\|E_{i\,T_{ij}}^{\,n}\|^2 - \sqrt{\frac{\mu_i}{\epsilon_i}}\,\|H_{i\,T_{ij}}^{\,n\text{-}1/2}\|^2\right]$$

$$=\; -\Delta t \sum_{\substack{\text{interfaces}}}^{\text{absorbing}} \|\vec{n}_{ij}\|\left[\sqrt{\frac{\epsilon_i}{\mu_i}}\left\| \frac{E_{i\,T_{ij}}^{\,n} + E_{i\,T_{ij}}^{\,n+1}}{2}\right\|^2 + \sqrt{\frac{\mu_i}{\epsilon_i}}\left\| \frac{H_{i\,T_{ij}}^{\,n\text{-}1/2} + H_{i\,T_{ij}}^{\,n+1/2}}{2}\right\|^2\right].$$

We have proved that the scheme (4-5-6-10) is such that the discrete energy $\mathcal{F}^n$ is non-increasing, hence it is bounded by its initial value. We can notice here that this result is valid independently of the value of the time step Δt.

4.3 A sufficient stability condition

In order to prove that our scheme is stable, we finally show that the discrete energy $\mathcal{F}^n$, under a stability condition on Δt, is a positive definite quadratic form of the numerical values $H_i^{n\text{-}1/2}$ and E_i^n. This leads to the result of this paper, taking the form of the following stability

THEOREM 4.1 *Using the scheme (4-5-6-10) on arbitrary polygonal finite volumes as described in this section, the energy $\mathcal{F}^n$ defined in (11) is a non-increasing, positive definite quadratic form of all unknowns $(E_i^n, H_i^{n\text{-}1/2})$, and therefore the scheme is L^2-stable, if the time step Δt is such that*

$$\forall \; interface \; a_{ij}, \; \Delta t^2 < 16 \; \frac{V_i V_j}{P_i P_j} \; \min(\epsilon_j \mu_i, \epsilon_i \mu_j),$$

(with the convention that j should be replaced by i in the above formula for boundary interfaces a_{ij}).

Proof: We get back to the definition of the discrete energy $\mathcal{F}^n$. We have

$$\mathcal{F}^n = \sum_i V_i \left(\epsilon_i \,{}^t\!E_i^n E_i^n + \mu_i \,{}^t\!H_i^{n\text{-}1/2} H_i^{n+1/2} \right) - \Delta t \sum_{\text{interfaces}}^{\text{absorbing}} \frac{\|\vec{n}_{ij}\|}{4} \left[\sqrt{\frac{\epsilon_i}{\mu_i}} \, \|E_{i T_{ij}}^n\|^2 - \sqrt{\frac{\mu_i}{\epsilon_i}} \, \|H_{i T_{ij}}^{n\text{-}1/2}\|^2 \right]$$

The magnetic field $H_i^{n+1/2}$ is given by (4) and depends linearly on $H_i^{n\text{-}1/2}$ and the fluxes G_{ij}^n. The latter depend linearly in all cases on the E_i^n and for the absorbing boundary on the $H_i^{n\text{-}1/2}$ through (10). Then it is clear that $\mathcal{F}^n$ and $\mathcal{E}^n$ as well are quadratic forms of the unknowns $(E_i^n, H_i^{n\text{-}1/2})$. We now need a lower bound for $\mathcal{F}^n$. We have

$$
\begin{aligned}
\mathcal{E}^n &= \sum_i V_i \left(\epsilon_i \,{}^t\!E_i^n E_i^n + \mu_i \,{}^t\!H_i^{n\text{-}1/2} H_i^{n+1/2} \right) \\[2mm]
&= \sum_i \left[V_i \epsilon_i \|E_i^n\|^2 + \mu_i V_i \|H_i^{n\text{-}1/2}\|^2 + \Delta t \,{}^t\!H_i^{n\text{-}1/2} \sum_{j \in \mathcal{V}_i} G_{ij}^n \right] \\[2mm]
&= \sum_i \left[V_i \epsilon_i \|E_i^n\|^2 + \mu_i V_i \|H_i^{n\text{-}1/2}\|^2 + \Delta t \,{}^t\!H_i^{n\text{-}1/2} \sum_{j \in \mathcal{V}_i} \left(G_{ij}^n - \frac{N_{ij}}{2} E_i^n \right) \right] \\[2mm]
&= \sum_i \sum_{j \in \mathcal{V}_i} \left[\frac{V_i \epsilon_i}{P_i} \|\vec{n}_{ij}\| \|E_i^n\|^2 + \frac{\mu_i V_i}{P_i} \|\vec{n}_{ij}\| \|H_i^{n\text{-}1/2}\|^2 + \Delta t \,{}^t\!H_i^{n\text{-}1/2} \left(G_{ij}^n - \frac{N_{ij}}{2} E_i^n \right) \right].
\end{aligned}
$$

In the above expression, the double summation over cells and cell neighbors can be redistributed over cell interfaces (internal interfaces will gather two contributions from neighboring cells, whereas boundary interfaces will gather only one inwards contribution). We then have

$$
\begin{aligned}
\mathcal{E}^n = \sum_{\text{interfaces}}^{\text{internal}} &\left[\frac{V_i \epsilon_i}{P_i} \|\vec{n}_{ij}\| \|E_i^n\|^2 + \frac{\mu_i V_i}{P_i} \|\vec{n}_{ij}\| \|H_i^{n\text{-}1/2}\|^2 + \frac{\Delta t}{2} \,{}^t\!H_i^{n\text{-}1/2} N_{ij} E_j^n \right. \\
&\left. + \frac{V_j \epsilon_j}{P_j} \|\vec{n}_{ij}\| \|E_j^n\|^2 + \frac{\mu_j V_j}{P_j} \|\vec{n}_{ij}\| \|H_j^{n\text{-}1/2}\|^2 - \frac{\Delta t}{2} \,{}^t\!H_j^{n\text{-}1/2} N_{ij} E_i^n \right] + \\
\sum_{\text{interfaces}}^{\text{metallic}} &\left[\frac{V_i \epsilon_i}{P_i} \|\vec{n}_{ij}\| \|E_i^n\|^2 + \frac{\mu_i V_i}{P_i} \|\vec{n}_{ij}\| \|H_i^{n\text{-}1/2}\|^2 - \frac{\Delta t}{2} \,{}^t\!H_i^{n\text{-}1/2} N_{ij} E_i^n \right] + \\
\sum_{\text{interfaces}}^{\text{absorbing}} &\left[\frac{V_i \epsilon_i}{P_i} \|\vec{n}_{ij}\| \|E_i^n\|^2 + \frac{\mu_i V_i}{P_i} \|\vec{n}_{ij}\| \|H_i^{n\text{-}1/2}\|^2 - \frac{\Delta t}{2} \|\vec{n}_{ij}\| \sqrt{\frac{\mu_i}{\epsilon_i}} \left\| H_{i T_{ij}}^{n\text{-}1/2} \right\|^2 \right].
\end{aligned}
$$

Using elementary minorations of scalar products, the definition of the matrix N_{ij} and adding correction terms in $\mathcal{F}^n$, we find that

$$
\begin{aligned}
\mathcal{F}^n \geq & \sum_{\substack{\text{internal} \\ \text{interfaces}}} \|\vec{n}_{ij}\| \left[\left(\frac{V_j \epsilon_j}{P_j} \|E_j^n\|^2 + \frac{\mu_i V_i}{P_i} \|H_i^{n-1/2}\|^2 - \frac{\Delta t}{2} \|H_i^{n-1/2}\| \|E_j^n\| \right) \right. \\
& \left. + \left(\frac{V_i \epsilon_i}{P_i} \|E_i^n\|^2 + \frac{\mu_j V_j}{P_j} \|H_j^{n-1/2}\|^2 - \frac{\Delta t}{2} \|H_j^{n-1/2}\| \|E_i^n\| \right) \right] + \\
& \sum_{\substack{\text{metallic} \\ \text{interfaces}}} \|\vec{n}_{ij}\| \left[\frac{V_i \epsilon_i}{P_i} \|E_i^n\|^2 + \frac{\mu_i V_i}{P_i} \|H_i^{n-1/2}\|^2 - \frac{\Delta t}{2} \|E_i^n\| \|H_i^{n-1/2}\| \right] + \\
& \sum_{\substack{\text{absorbing} \\ \text{interfaces}}} \|\vec{n}_{ij}\| \left[\frac{V_i \epsilon_i}{P_i} \|E_i^n\|^2 + \frac{\mu_i V_i}{P_i} \|H_i^{n-1/2}\|^2 - \frac{\Delta t}{4} \sqrt{\frac{\mu_i}{\epsilon_i}} \left\| H_{i_{T_{ij}}}^{n-1/2} \right\|^2 - \frac{\Delta t}{4} \sqrt{\frac{\epsilon_i}{\mu_i}} \left\| E_{i_{T_{ij}}}^n \right\|^2 \right]
\end{aligned}
$$

Thus, if all discriminants are strictly negative, i.e. the time step Δt is such that

$$
\begin{cases}
i) & \forall \text{ internal interface } a_{ij}, \quad \Delta t^2 < 16 \, \frac{V_i V_j}{P_i P_j} \, \min(\epsilon_j \mu_i, \epsilon_i \mu_j), \\
ii) & \forall \text{ metallic interface near cell } \mathcal{C}_i, \qquad \Delta t < 4 \, \frac{V_i}{c_i P_i}, \\
iii) & \forall \text{ absorbing interface near cell } \mathcal{C}_i, \qquad \Delta t < 4 \, \frac{V_i}{c_i P_i},
\end{cases}
$$

it is clear that $\mathcal{F}^n \geq 0$ and that $\mathcal{F}^n = 0 \Rightarrow (\forall \, i, \quad E_i^n = 0, H_i^{n-1/2} = 0)$. This concludes the proof that under the condition of Theorem 4.1, the discrete energy $\mathcal{F}^n$ is a positive definite quadratic form of all numerical unknowns. It is also non-increasing, then bounded and the scheme is L^2-stable.

REMARK 4.1 *Comparison with Yee's scheme*

The comparison of the sufficient stability condition given in Theorem 4.1 with the stability limit obtained by a Von Neumann analysis of Fourier eigenmodes for a structured orthogonal regular grid yields an estimation of the optimality of this sufficient condition. For an orthogonal Cartesian grid made of square hexahedra $\Delta x \times \Delta y \times \Delta z$, Remaki [19] has proven that the centered finite volume scheme (for an homogeneous medium) is stable if and only if

$$
c\Delta t \sqrt{\frac{1}{\Delta x^2} + \frac{1}{\Delta y^2} + \frac{1}{\Delta z^2}} \leq 2,
$$

which makes possible the use of a time step twice bigger than with Yee's scheme [30] (see [26] for a correct proof). For the same Cartesian grid, our general sufficient stability condition is

$$
c\Delta t \left(\frac{1}{\Delta x} + \frac{1}{\Delta y} + \frac{1}{\Delta z} \right) \leq 2,
$$

which is more restrictive, but note that it is only sufficient and not necessary. Although the new FVTD scheme with a twice finer grid recovers the same stability limit and dispersion as Yee's scheme, the main property of this scheme is its ability to handle complex geometries using unstructured grids. In the sequel, some numerical results show the basic property of the scheme, including on unstructured grids around complex geometries.

5 Numerical results

5.1 A rectangular waveguide with a current source (2D)

We consider a current j_z over the cross section of a rectangular waveguide at $x = 0$ (see Figure 2), given by $j_z(y) = \sqrt{2} \sin(\pi y/d) \cos(2\pi f t)$, where $d = 1$m is the waveguide width and $f = 0.3$Ghz the signal frequency. The grid used here corresponds to 12 points per wavelength. Figure 3 and Figure 4 represent the electric and the magnetic fields produced by the current j_z. We can see on Figure 3 the good quality of the approximate solutions, which compare very well with exact solutions.
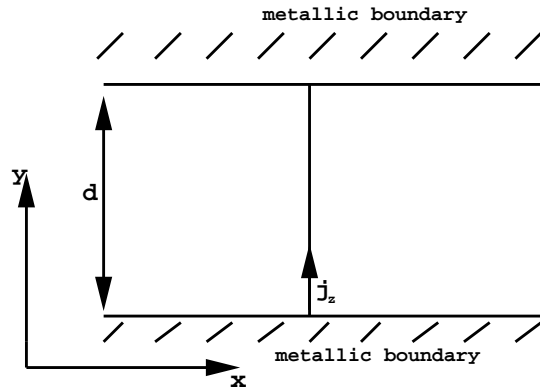
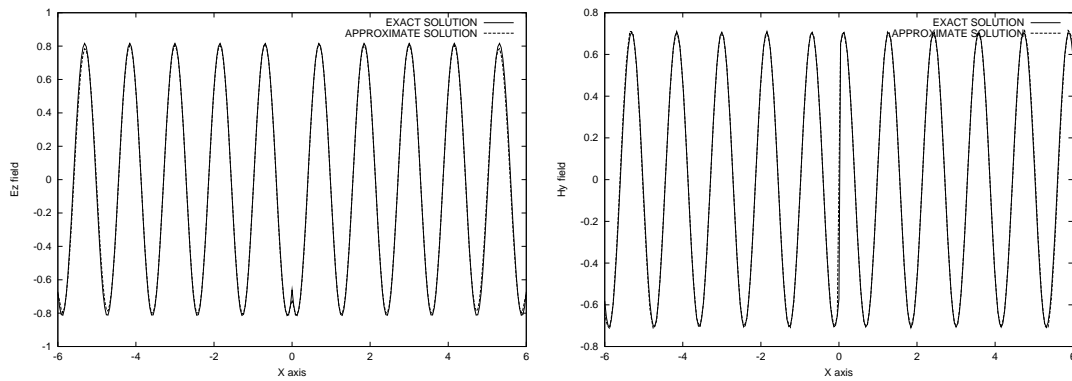Figure 2: A current sheet in a rectangular waveguide

Figure 3: Section at y=$\frac{d}{2}$, E_z (left) and H_y (right). Numerical and exact solutions.
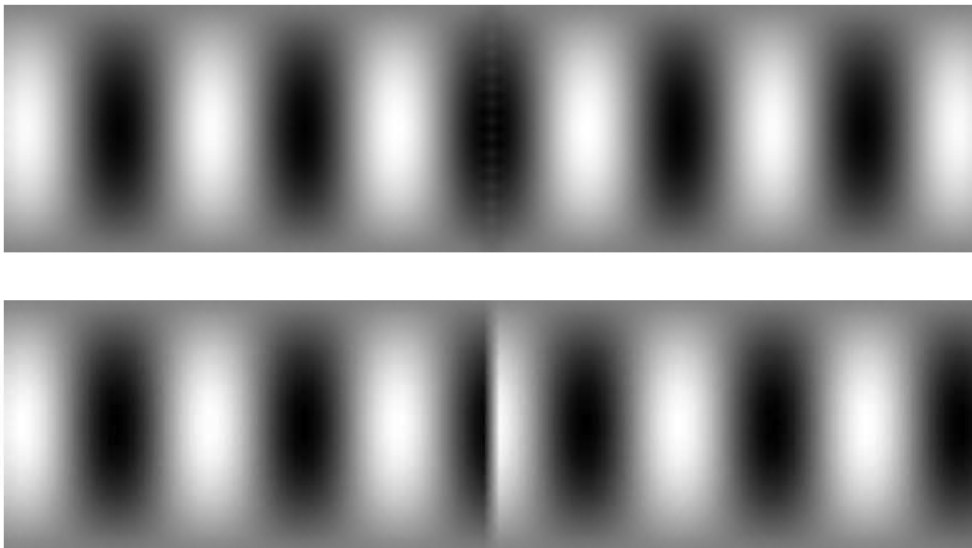

Figure 4: Numerical E_z (above) and H_y (down).

5.2 Scattered waves across a dielectric coated airfoil (2D)

We simulate scattering problems across airfoils in heterogeneous cases. We first illuminate a coated NACA0012 airfoil profile (dielectric layer of thickness $\delta = 0.1\lambda$, with $\varepsilon = 4$ and μ=1) by a monochromatic

11

wave located rightwards (with frequency $f = 1.2\text{Ghz}$). The space discretization is unstructured and corresponds to 15 points per wavelength (see Figure 5). Figure 6 represents the contours of the scattered electric field. We can notice that the numerical solution has no spurious oscillation at the interface between the two materials.

5.3   Scattered waves across a coated cylinder (2D)

We present here as an example the computed result for the magnetic field scattered by a model antenna (here an heterogeneous circular dielectric cylinder scatterer), which is pictured on Figure 7.The frequency of the incident wave coming from the right side of the object is $f = 0.15\text{Ghz}$. The radius of the large metallic cylinder is $R = 0.459\text{m}$, while the radius of small metallic cylindrical inclusions is $R = 0.025\text{m}$ (the centers are regularly spaced with an interval of 0.1m) , the thickness of the dielectric layer is $\delta = 0.1\text{m}$. The perfect dielectric material is defined by $\varepsilon_r = 2.56$ and $\mu_r = 1$. In this test case, the mesh is rather coarse, since we have only 14 points per wavelength.

5.4   Electromagnetic compatibility

We consider an airfoil's window with a slit as in Figure 8. The relative parameters of the dielectric layer are $\varepsilon_r = 2$ and $\mu_r = 1$. We consider different imperfectly conducting materials (different σ). We send a monochromatic wave with incidence angle $\theta = 90^o$, and frequency $f = 0.3Ghz$. We compute the wave propagation across the material (Figures 9 and 10). These simulations were produced with an exponential time scheme for the treatment of the additional loss terms. Depending on the conductivity σ of the non perfect conductor, we get different total electric field with a smooth transition from an apparent perfect dielectric ($\sigma = 0$) to an almost symmetric solution (for $\sigma = 100$, we have almost two perfect conductors).

5.5   Eigenmodes in a three-dimensional metallic cavity

We present here preliminary results for the numerical simulation of the time evolution of an eigenmode in a cubic metallic cavity, We consider the (1,1,1) mode. The cubic cavity is discretized by a structured orthogonal regular cubes, with twenty cells in each direction. We have chosen to present on Figure 11 the vertical component H_z of the magnetic field at the center of the cavity in function of the time. Numerical results obtained by Yee's scheme and our finite volume scheme (with cubic elementary volumes) are comparable : no numerical dissipation is artificially produced and the L^2 error with the exact solution (pointwise differences for both grids) is very small. For each numerical scheme, we have plotted the exact and approximate value corresponding to the considered degree of freedom. Since Yee's scheme involves a staggered grid, both "exact" curves differ. We can observe that, on this particular case of
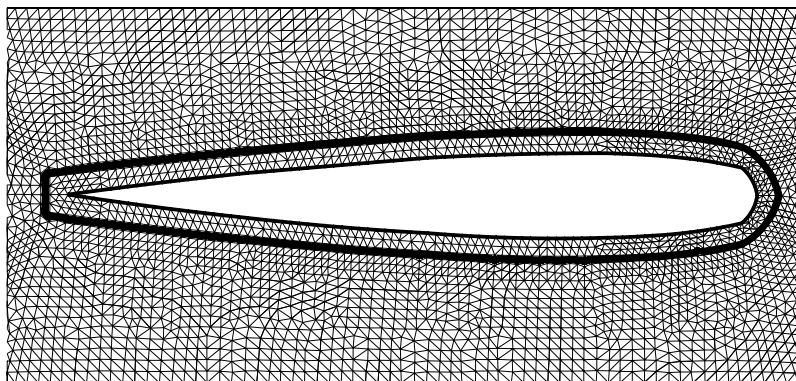

Figure 5: The unstructured discretization for the coated NACA0012 airfoil (the dielectric material corresponds to triangles inside the marked line).
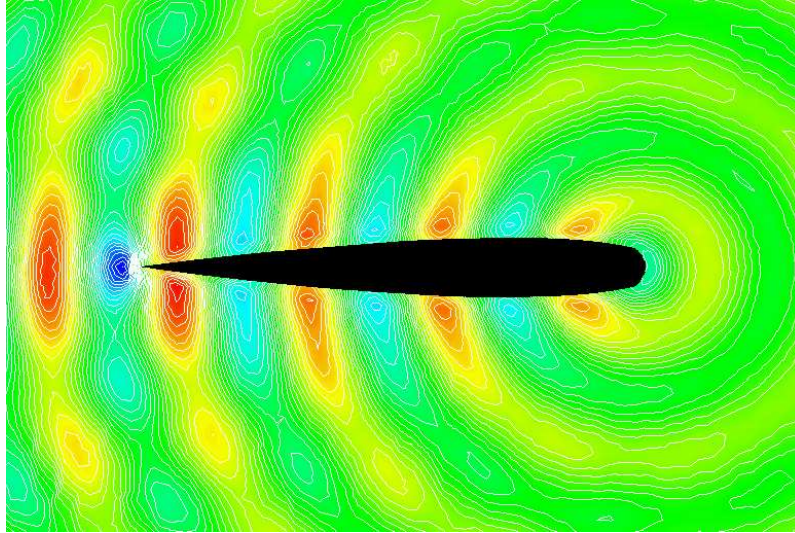
Figure 6: The scattered electric field

a regular orthogonal grid, the numerical dispersions and the computational costs of both FVTD and FDTD methods are comparable.

6   Conclusion

In this paper, we have proposed a sufficient condition for the stability of the second order finite volume scheme proposed by Remaki for the time domain solution of Maxwell equations in two and three dimensions in heterogenous media. Energy estimates lead us to a sufficient CFL-like stability conditions on arbitrary finite volumes with metallic or absorbing boundary conditions, for which weak treatments with at least consistent numerical fluxes have been used. The stability condition happens to be more restrictive – but with a comparable limit time step – on regular grids than that obtained with Fourier analysis. However, this condition is general. Some numerical results in two and three dimensions proved the large potential of the method, for which several works are still ahead: proof of convergence and second-order accuracy on unstructured grids, coupling with PML medium, multi-scale coupling of multiple subdomains with different mesh sizes and time steps.

References

[1] D.A. Anderson, J.C. Tannehill, and R.H. Pletcher. *Computational fluid mechanics and heat transfer.* Hemisphere. McGraw-Hill, New York, 1984.

[2] Jean-David Benamou and Bruno Despres. A domain decomposition method for the helmholtz equation and related optimal control problems. *J. Comput. Phys.*, 136(1):68–82, 1997.

[3] F. Bourdel, P.-A. Mazet, and Helluy. P. *Resolution of the non-stationary or harmonic Maxwell equations by a discontinuous finite element method. Application to an E.M.I. (electromagnetic impulse) case*, pages 405–422. Computing Methods in Applied Sciences and Engineering. Nova Science Publishers, Inc., New-York, 1991.

[4] J.P. Brenger. Three-dimensional perfectly matched layer for the absorption of electromagnetic waves. *J. Comput. Phys.*, 127:363–379, 1996.

[5] P. G. Ciarlet and J.-L. Lions, editors. *Handbook of Numerical Analysis*, volume 1/2. North Holland-Elsevier Science Publishers, Amsterdam, New York, Oxford, 1991.
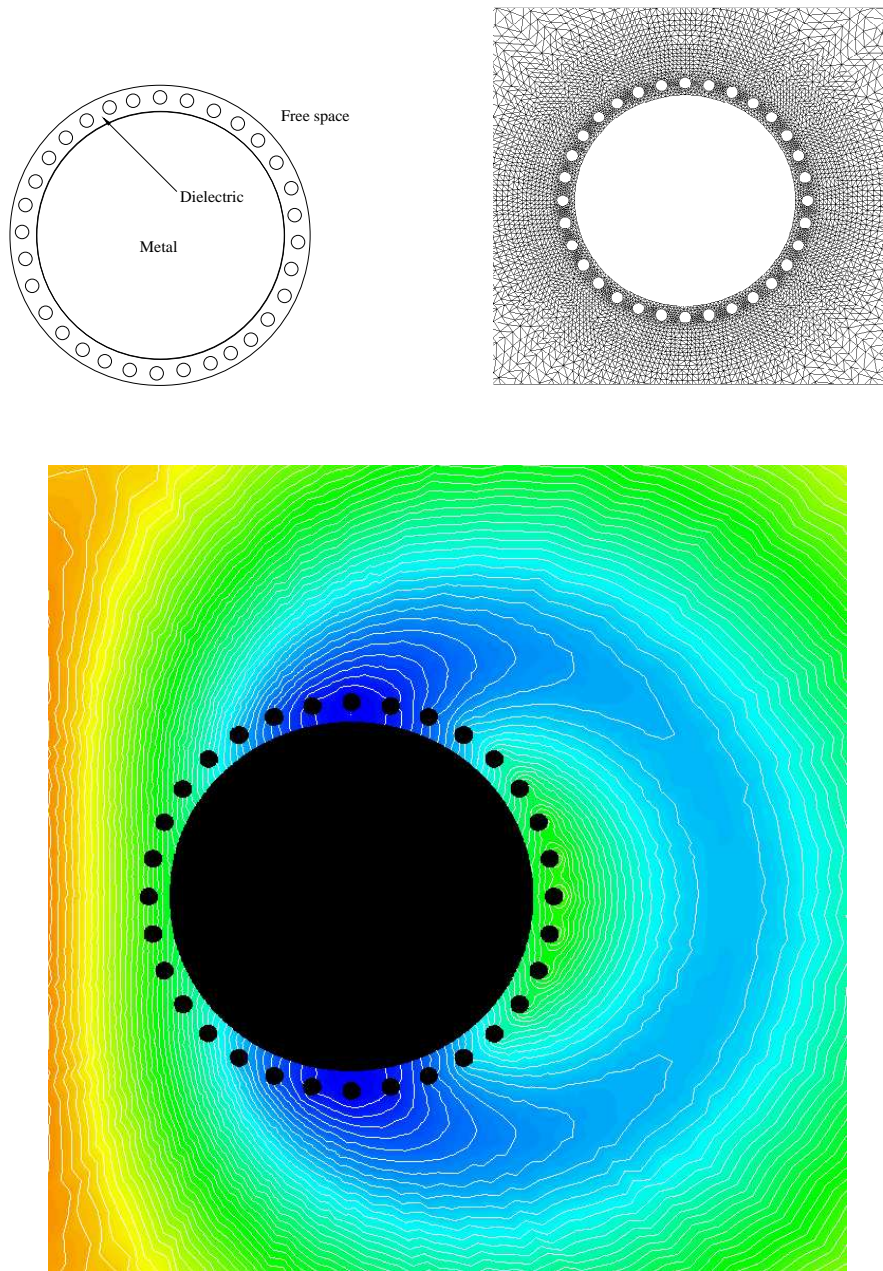
Figure 7: Geometry(above, left), zoom of the mesh (above, right) and scattered magnetic field (down).
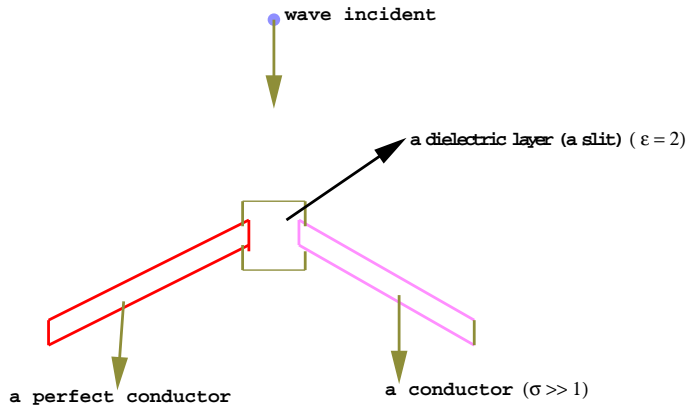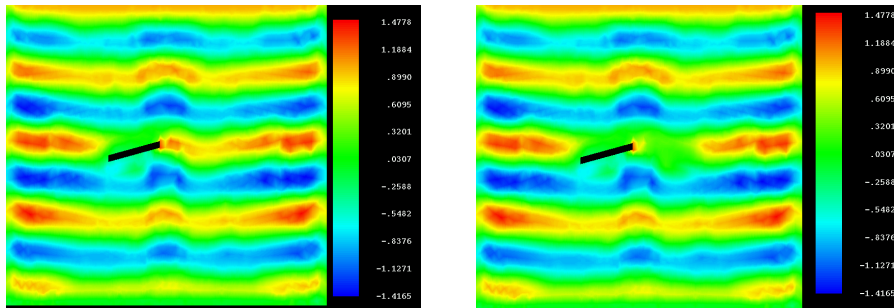
Figure 8: a window's slit

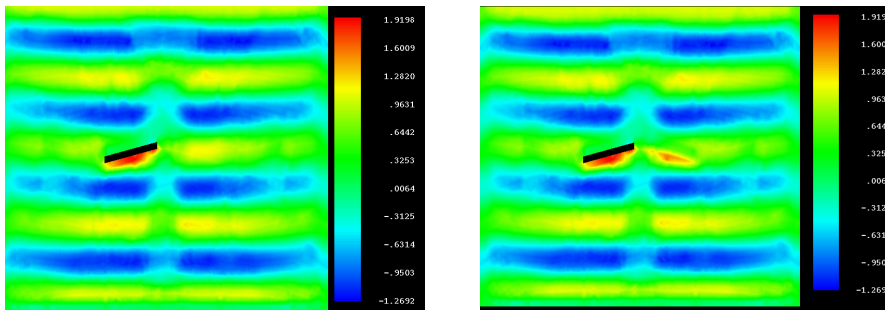Figure 9: Total electric field - $\sigma = 0$ (left) and $\sigma = 100$ (right)

Figure 10: Total magnetic field - $\sigma = 0$ (left) and $\sigma = 100$ (right)

[6] J.-P. Cioni, L. Fezoui, and H. Steve. Approximation des quations de Maxwell par des schmas dcentrs en lments finis. Technical Report RR-1601, INRIA, February 1992.

[7] J.-P. Cioni and M. Remaki. Comparaison de deux mthodes de volumes finis en electromagntisme. Technical Report RR-3166, INRIA, May 1997.

[8] Jean-Pierre Cioni, L. Fezoui, L. Anne, and F. Poupaud. A parallel FVTD Maxwell solver using 3d unstructured meshes. In *13th annual review of progress in applied computational electromagnetics*, Monterey, California, 1997.

[9] G. Cohen and P. Joly, editors. *Aspects rcents en mthodes numriques pour les quations de Maxwell*, Collection didactique INRIA, INRIA Rocquencourt, France, March 23-27 1998.

[10] Francis Collino and Peter Monk. The perfectly matched layer in curvilinear coordinates. *SIAM J. Sci. Comput.*, 19(6):2061–2090, 1998.
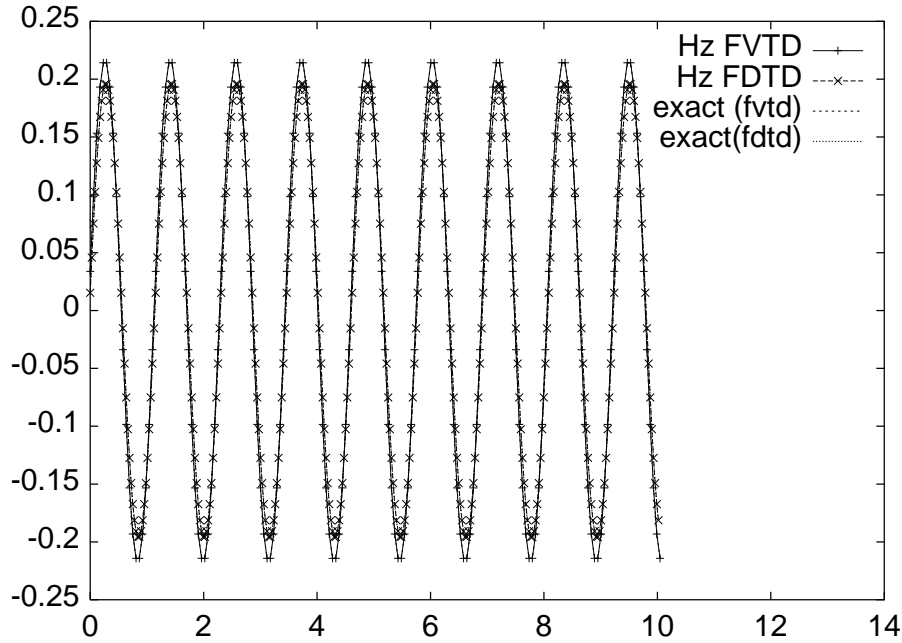
Figure 11: Vertical magnetic field at the center of a metallic cubic cavity for Yee's scheme and our finite volume scheme

[11] R. Eymard, T. Gallout, and R. Herbin. *The finite volume method.* to appear in Handbook for Numerical Analysis. North Holland-Elsevier Science Publishers, Amsterdam, New York, Oxford, 1999.

[12] A. Harten. High Resolution Schemes for Hyperbolic Conservation Laws. *J. Comput. Phys.*, 49:357–393, 1983.

[13] A. Jameson. Artificial diffusion, upwind biasing, limiters and their effect on accuracy and multigrid convergence in transonic and hypersonic flows. In *11th AIAA Computational Fluid Dynamics Conference, Orlando, Florida*, July 6-9 1993. AIAA paper 93-3359.

[14] P. Lesaint. *Sur la rsolution des systmes hyperboliques du premier ordre par des mthodes d'lments finis.* PhD thesis, Universit de Paris VI, 1975.

[15] Michael F. Pasik, David B. Seidel, and Raymond W. Lemke. A modified perfectly matched layer implementation for use in electromagnetic pic codes. *J. Comput. Phys.*, 148(1):125–132, 1999.

[16] Peter G. Petropoulos. On the termination of the perfectly matched layer with local absorbing boundary conditions. *J. Comput. Phys.*, 143(2):665–673, 1998.

[17] S. Piperno. L^2-stability of the upwind first order finite volume scheme for the maxwell equation in two and three dimensions on arbitrary unstructured meshes. *RAIRO Modél. Math. Anal. Numér.*, 34(1):139–158, 2000.

[18] F. Poupaud and M. Remaki. Existence and uniqueness of the maxwell's system solutions in heterogeneous and irregular media. *C. R. Acad. Sci. Paris Sér. I Math.*, t. 330:99–103, 2000.

[19] M. Remaki. A new finite volume scheme for solving maxwell's system. *COMPEL- The International Journal for Computation and Mathematics in Electric and Electronic Engineering*, 19(3):913–931, 2000.

[20] M. Remaki, L. Fezoui, and F. Poupaud. Un nouveau schma de type volumes finis appliqu aux quations de Maxwell en milieu htrogne. Technical Report RR-3351, INRIA, January 1998.

16

[21] J.S. Shang. A characteristic-based algorithm for solving 3d, time-domain Maxwell equations. In *30th Aerospace Sciences Meeting and Exhibit*, Reno, Nevada, January 6-9 1992. AIAA paper 92-0452.

[22] J.S. Shang and R.M. Fithen. A comparative study of characteristic-based algorithms for the Maxwell equations. *J. Comput. Phys.*, 125:378–394, 1996.

[23] V. Shankar, W.F. Hall, and A.H. Mohammadian. A time-domain differential solver for electromagnetic scattering problems. *Proc. IEEE*, 77(5):709–720, 1989.

[24] A. Taflove. Re-inventing electromagnetics: supercomputing solution of Maxwell's equations via direct time integration on space grids. AIAA paper 92-0333, 1992.

[25] A. Taflove. *Computational electrodynamics : the finite-difference time-domain method.* Artech house, 1995.

[26] A. Taflove and E. Brodwin. Numerical solution of steady-state electromagnetic scattering problems using the time-dependent maxwell's equations. *IEEE Trans. Microwave Theory Tech.*, MTT-23:623–630, 1975.

[27] J.-P. Vila. Convergence and error estimates in finite volume schemes for general multidimensional scalr conservation laws. I. explicite monotone schemes. *RAIRO Modél. Math. Anal. Numér.*, 28(3):267–295, 1994.

[28] J.-P. Vila and P. Villedieu. Convergence de la méthode des volumes finis pour les systèmes de Friedrichs. *C. R. Acad. Sci. Paris Sér. I Math.*, 3(325):671–676, 1997.

[29] R.F. Warming and F. Hyett. The modified equation approach to the stability and accuracy analysis of finite-difference methods. *J. Comput. Phys.*, 14(2):159–179, 1974.

[30] K. S. Yee. Numerical solution of initial boundary value problems involving Maxwell's equations in isotropic media. *IEEE Trans. Antennas and Propagation*, (AP-16):302–307, 1966.